Journal of Electrotechnology, Electrical Engineering and Management (2026)
Clausius Scientific Press, Canada
DOI: 10.23977/jeeem.2026.090103
ISSN 2560-6697 Vol. 9 Num. 1

Study on Temperature Compensation Techniques for Silicon Piezoresistive Pressure Sensors under Rapid Temperature Variations

Xinshi Zhang[1,*], Lijun Yang[1], Songli Wang[2], Xiongkai Dang[1]

[1]School of Mechanical and Electrical Engineering, Shaanxi University of Science and Technology, Xi'an, China
[2]Xi'an Siwei Sensing Technology Co., Ltd, Xi'an, China
**Corresponding author: zhangxinshi2023@163.com*

Keywords: Silicon Piezoresistive Pressure Sensor, Temperature Compensation, Rapid Temperature Variation

Abstract: To address the issue of output jumps and reduced accuracy in silicon piezoresistive pressure sensors caused by the mismatch of thermal expansion coefficients among different structural components under rapid cooling conditions, this study investigates a temperature compensation algorithm tailored for such operating environments. Firstly, the influence mechanism of temperature on the output characteristics of the pressure sensor was analyzed, and calibration experiments were conducted within the sensor's operating range (10–60 °C). Subsequently, rapid cooling experiments were performed using calibration parameters obtained from different temperature trajectories, and the effects of various compensation methods on output accuracy were compared. The experimental results indicate that, compared with compensation methods based solely on either the heating or cooling calibration parameters, the proposed method, which combines calibration parameters from both heating and cooling trajectories, can effectively reduce output jumps and improve the stability and accuracy of the sensor under rapid temperature variations.

1. Introduction

Pressure sensors, as key components for measuring gas and liquid pressures, have been widely applied in aerospace, automotive electronics, industrial process control, and medical devices. Among them, piezoresistive pressure sensors, which feature simple structures, high sensitivity, and fast dynamic response, are the most extensively used[1-3].

In silicon piezoresistive pressure sensors, the pressure-sensitive chip is primarily made of semiconductor materials. Due to its temperature sensitivity and limitations in fabrication processes, issues such as temperature drift and temperature hysteresis are commonly observed. Temperature drift arises from changes in bridge resistance caused by temperature variations, leading to abnormal output, and is typically corrected via temperature compensation algorithms. Temperature hysteresis manifests as inconsistent outputs at the same pressure point under identical temperatures during heating and cooling, mainly due to differences in the thermal expansion coefficients of various structural

components in the pressure chip. This results in nonlinear and lagged behavior during temperature changes, causing the sensor output to depend on the direction of temperature variation[4-6].

Currently, temperature compensation algorithms primarily compensate for temperature drift by establishing the relationship among temperature, measured output pressure, and reference pressure. Temperature hysteresis is generally mitigated by selecting materials with similar thermal expansion coefficients. However, due to the inherent limitations of structural materials in the chip, it is impossible to perfectly match the thermal expansion coefficients of all components, and hysteresis cannot be completely eliminated[7]. The effect is particularly pronounced under rapid temperature variations, where pressure outputs change more significantly. In practical tests, rapid drops in ambient temperature can lead to inconsistent outputs at the same pressure points. To address these issues, this study proposes a compensation algorithm aimed at reducing the impact of rapid temperature variations on output accuracy.

2. Experimental Setup and Principles of the Compensation Algorithm

2.1 Experimental Procedure

Prior to use, pressure sensors typically require calibration. Within the operating temperature range, a series of temperature points is set at fixed increments, and the sensor is held at each temperature point in a temperature chamber to acquire pressure data for calibration. Traditionally, compensation models are established using either heating or cooling calibration data. However, in practical applications, it has been observed that when the ambient temperature varies rapidly, temperature compensation based solely on a single heating or cooling dataset exhibits reduced accuracy.

For instance, in a certain test environment, the pressure sensor experiences the following stages during operation:

(1) Heating Stage: After power-up, the sensor temperature rises due to heating from the PCB CPU and environmental influences. Testing is performed once thermal equilibrium is reached and the output stabilizes.

(2) Cooling Stage: During testing, the sensor temperature may drop rapidly due to environmental factors, leading to corresponding changes in the output pressure.

(3) Thermal Equilibrium Stage: After some time, the sensor reaches thermal equilibrium, and the pressure output stabilizes

Under these conditions, the trends of sensor temperature and zero-point output are shown in Figure 1.

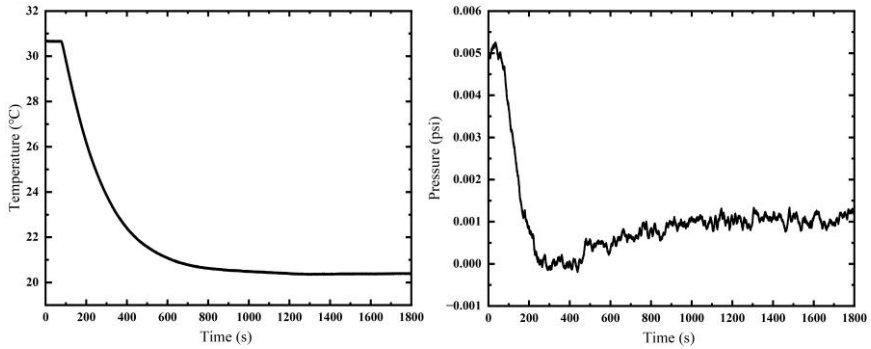

(a) (b)

Figure 1. (a) Temperature variations of the pressure sensor during operation; (b) Zero-point output variations of the pressure sensor during operation

As shown in Figure 1(b), the output of the pressure sensor initially decreases and then stabilizes

during rapid cooling. After the output stabilizes, significant differences remain between pre- and post-cooling outputs due to temperature hysteresis. To reduce temperature hysteresis error, i.e., the output difference before and after cooling, the following methods for establishing compensation models are proposed:

(1) Compensation Model Based on Heating Calibration Data

Calibration data obtained during the temperature increase from 10 °C to 60 °C are fitted to establish a temperature compensation model.

(2) Compensation Model Based on Cooling Calibration Data

Calibration data obtained during the temperature decrease from 60 °C to 10 °C are fitted to establish a temperature compensation model.

(3) Compensation Model Based on Combined Heating–Cooling Calibration Data

Considering the actual operating conditions of the pressure sensor, as illustrated in Figure 1(a), the sensor reaches a thermal equilibrium temperature of approximately 30 °C after power-up, at which point the output corresponds to the heating trajectory. After experiencing cooling, thermal equilibrium is reached again at approximately 20 °C, corresponding to the output during cooling. Therefore, calibration data at 10 °C and 20 °C from the cooling trajectory, as well as 30 °C, 40 °C, 50 °C, and 60 °C from the heating trajectory, are selected to establish the compensation model.

2.2 Principles of the Compensation Algorithm

The compensation algorithm employs a polynomial-based approach, and its principle is as follows:

Since an n-th order polynomial can approximate any continuous function over a closed interval, the input-output relationship of the pressure sensor within its full-scale range [$P_{\min}$,$P_{\max}$] at a given fixed temperature can be expressed by a polynomial function:

$$P_0 = \sum_{i=0}^{N} a_i U^i = a_0 + a_1 U + a_2 U^2 + \cdots + a_N U^N \tag{1}$$

In Equation (1), P_0 denotes the applied reference pressure, and U represents the output voltage of the pressure sensor.

Due to the influence of temperature, the coefficients a_i in Equation (1) vary with temperature. That is, a_i can be considered as a function of temperature T, and it can also be approximated by a polynomial function:

$$a_i(T) = \sum_{j=0}^{M} b_{ji} T^j = b_{0i} + b_{1i} T + b_{2i} T^2 + \cdots + b_{Mi} T^M \tag{2}$$

The final output can be expressed as:

$$P_0 = \sum_{i=0}^{N} a_i(T) U^i = \sum_{i=0}^{N} \sum_{j=0}^{M} b_{ji} T^j U^i \tag{3}$$

By substituting the calibration data into Equation (3), the coefficients b_{ji} can be determined through curve fitting, thereby establishing the compensation model.

3. Full-Temperature-Range Calibration Experiments

Calibration experiments were conducted over the full temperature range of the pressure sensor. The experimental procedure is described as follows:

(1) Pneumatic Connection:

The pneumatic circuit of the pressure sensor was connected such that the pressure output line of the pressure controller was linked to the positive pressure input port of the sensor, while the reference port of the controller was connected to the reference port of the sensor. The reference port was exposed to atmospheric pressure. After verifying the airtightness of the pneumatic system, the sensor was placed inside a temperature chamber.

(2) Temperature Setting:

Within the heating interval (10 ℃ to 60 ℃) and the cooling interval (60 ℃ to 10 ℃), eleven standard temperature points, denoted as T_i,were set with a step size of 10 ℃. To ensure thermal equilibrium between the sensor and the temperature chamber, the sensor was maintained at each temperature point for 1.5 h before pressure data acquisition.

(3) Pressure Setting:

Within the pressure range of −2.5 psi to 2.5 psi (gauge pressure), nine standard pressure points, denoted as P_i, were set with a step size of 0.625 psi. After thermal equilibrium was achieved at each temperature point, pressure data were collected. To reduce the influence of pressure hysteresis error, the pressure value at each temperature point was obtained by averaging the data from the increasing and decreasing pressure trajectories.

Taking Sensor No. 1 as an example, its calibration data are presented in Table 1.

Table 1. Calibration Data of Sensor No. 1 over the Full Temperature Range

T_1/°C	U_1/mV								
	-2.5psi	-1.875psi	-1.25psi	-0.625psi	0psi	0.625psi	1.25psi	1.875psi	2.5psi
10	-77.652	-55.782	-33.924	-12.094	9.713	31.493	53.218	74.903	96.531
20	-76.912	-55.468	-34.039	-12.628	8.760	30.118	51.425	72.692	93.903
30	-76.131	-55.105	-34.077	-13.069	7.910	28.865	49.783	70.646	91.463
40	-75.304	-54.644	-33.998	-13.384	7.209	27.770	48.294	68.776	89.209
50	-74.391	-54.105	-33.836	-13.582	6.643	26.841	47.007	67.123	87.197
60	-73.446	-53.514	-33.606	-13.709	6.169	26.010	45.823	65.583	85.311
50	-74.440	-54.156	-33.891	-13.637	6.585	26.776	46.933	67.059	87.124
40	-75.366	-54.716	-34.076	-13.459	7.142	27.712	48.228	68.717	89.149
30	-76.210	-55.168	-34.145	-13.139	7.837	28.782	49.694	70.550	91.374
20	-76.974	-55.535	-34.107	-12.700	8.682	30.023	51.331	72.591	93.805
10	-77.663	-55.796	-33.934	-12.101	9.713	31.478	53.206	74.894	96.529

4. Rapid Cooling Experiment

To evaluate the compensation performance of different temperature compensation models under practical operating conditions, targeted validation experiments were conducted on the pressure sensor after calibration. The test procedure was designed to closely replicate the actual operational process, thereby simulating the temperature variations encountered in engineering applications.

Prior to testing, the pressure sensor was powered on and operated in a stationary environment without external airflow disturbance for 1.5 h. The output of the temperature sensor was monitored until the internal temperature reached a relatively stable thermal equilibrium state. After confirming thermal equilibrium, zero calibration was performed to eliminate the influence of initial zero-offset on subsequent test results.

After zero adjustment, external cooling conditions were introduced to simulate the temperature variations experienced by the sensor during the actual testing phase. The pressure sensor was continuously cooled using a temperature-controlled chamber set to 20 °C, allowing the overall sensor

temperature to gradually decrease from its thermal equilibrium state. During the entire cooling process, the pressure controller was set to 0 psi, ensuring that all sensors remained under zero-input conditions. This configuration enabled direct evaluation of the impact of temperature variations on zero-point stability and the effectiveness of the compensation models.

Throughout the cooling process, the sensor output signals were continuously acquired. The cooling duration was set to 1800 s, and the three compensation methods described in Section 2.1 were applied separately for comparative analysis.

5. Experimental Results

(1) Test Results Using the Compensation Model Based on Heating Calibration Data

The heating calibration data for Sensor No. 1 are presented in Table 2.

Table 2. Calibration Data of Sensor No. 1 Based on Heating Trajectory

T_1/°C	U_1/mV								
	-2.5psi	-1.875psi	-1.25psi	-0.625psi	0psi	0.625psi	1.25psi	1.875psi	2.5psi
10	-77.652	-55.782	-33.924	-12.094	9.713	31.493	53.218	74.903	96.531
20	-76.912	-55.468	-34.039	-12.628	8.760	30.118	51.425	72.692	93.903
30	-76.131	-55.105	-34.077	-13.069	7.910	28.865	49.783	70.646	91.463
40	-75.304	-54.644	-33.998	-13.384	7.209	27.770	48.294	68.776	89.209
50	-74.391	-54.105	-33.836	-13.582	6.643	26.841	47.007	67.123	87.197
60	-73.446	-53.514	-33.606	-13.709	6.169	26.010	45.823	65.583	85.311

The compensation model was established by substituting the data from Table 2 into Equation (3) and was implemented in the pressure sensor for the cooling experiment. The sensor outputs during the experiment are shown in Figure 2.

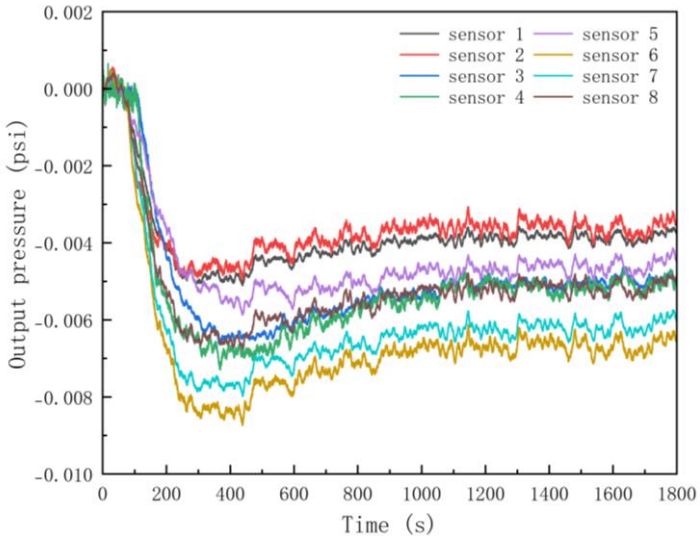

Figure 2. Sensor outputs during the cooling experiment using the compensation model based on heating calibration data

(2) Test Results Using the Compensation Model Based on Cooling Calibration Data

The cooling calibration data for Sensor No. 1 are presented in Table 3.

The compensation model was established by substituting the data from Table 3 into Equation (3) and implemented in the pressure sensor for the cooling experiment. The sensor outputs during the experiment are shown in Figure 3.

Table 3. Calibration Data of Sensor No. 1 Based on Cooling Trajectory

T_1/°C	U_1/mV								
	-2.5psi	-1.875psi	-1.25psi	-0.625psi	0psi	0.625psi	1.25psi	1.875psi	2.5psi
60	-73.446	-53.514	-33.606	-13.709	6.169	26.010	45.823	65.583	85.311
50	-74.440	-54.156	-33.891	-13.637	6.585	26.776	46.933	67.059	87.124
40	-75.366	-54.716	-34.076	-13.459	7.142	27.712	48.228	68.717	89.149
30	-76.210	-55.168	-34.145	-13.139	7.837	28.782	49.694	70.550	91.374
20	-76.974	-55.535	-34.107	-12.700	8.682	30.023	51.331	72.591	93.805
10	-77.663	-55.796	-33.934	-12.101	9.713	31.478	53.206	74.894	96.529

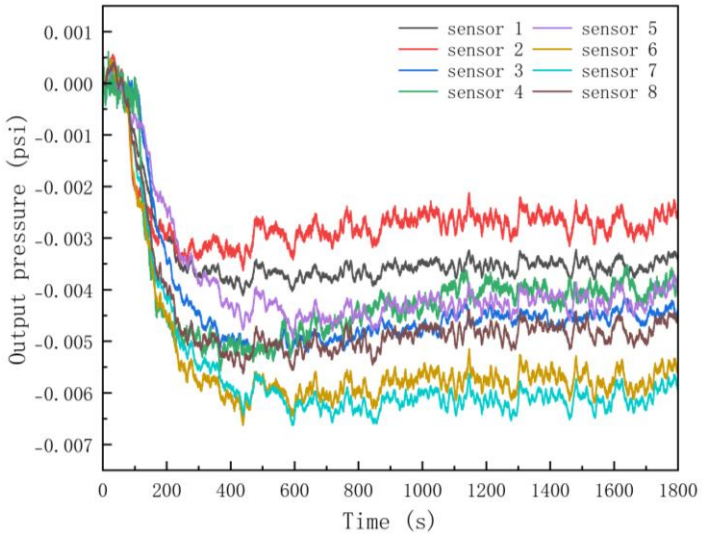

Figure 3. Sensor outputs during the cooling experiment using the compensation model based on cooling calibration data

(3) Test Results Using the Compensation Model Based on Combined Heating–Cooling Calibration Data

The combined heating–cooling calibration data are presented in Table 4.

Table 4. Combined Calibration Data: Cooling from 10–20 °C and Heating from 30–60 °C

T_1/°C	U_1/mV								
	-2.5psi	-1.875psi	-1.25psi	-0.625psi	0psi	0.625psi	1.25psi	1.875psi	2.5psi
10	-77.663	-55.796	-33.934	-12.101	9.713	31.478	53.206	74.894	96.529
20	-76.974	-55.535	-34.107	-12.700	8.682	30.023	51.331	72.591	93.805
30	-76.131	-55.105	-34.077	-13.069	7.910	28.865	49.783	70.646	91.463
40	-75.304	-54.644	-33.998	-13.384	7.209	27.770	48.294	68.776	89.209
50	-74.391	-54.105	-33.836	-13.582	6.643	26.841	47.007	67.123	87.197
60	-73.446	-53.514	-33.606	-13.709	6.169	26.010	45.823	65.583	85.311

The compensation model was established by substituting the data from Table 4 into Equation (3) and implemented in the pressure sensor for the cooling experiment. The sensor outputs during the experiment are shown in Figure 4.

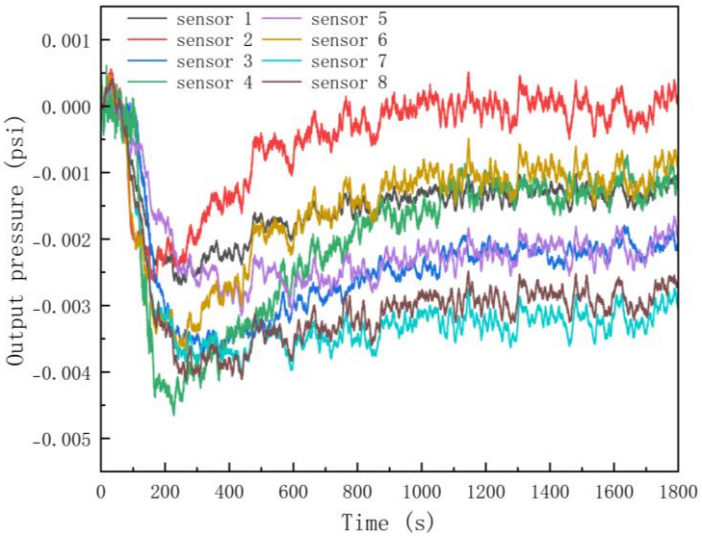

Figure 4. Sensor outputs during the cooling experiment using the compensation model based on combined heating–cooling calibration data

6. Conclusion

The experimental data presented in Section 5 were processed to calculate the steady-state output P_s, full-scale error (γ), and root-mean-square error (RMSE) for eight pressure sensors using the three compensation models. The steady-state output is defined as the pressure output after the sensor temperature stabilizes following cooling, calculated as the average of the last 100 pressure points during the test.

The full-scale error is calculated as follows:

$$\gamma = \frac{|P_s - P_0|}{P_{FS}} \times 100\% \tag{4}$$

In Equation (4),P_0 denotes the input pressure of the sensor,and P_{FS} represents the full-scale value of the sensor.

The root-mean-square error (RMSE) is calculated as follows:

$$RMSE = \sqrt{\sum_{i=1}^{n} \frac{(P_i - P_0)^2}{n}} \tag{5}$$

In Equation (5),P_i represents the data of the last 100 pressure points during the test,and n is therefore set to 100.

The errors of the test results using the three compensation methods are shown in Figures 5, 6, and 7.

As shown in Figure 5, during the cooling experiment, the sensors using the compensation model based on combined heating–cooling calibration data exhibited steady-state outputs closer to the reference pressure of 0 psi. Figure 6 indicates that, in terms of full-scale error, the cooling experiment using the combined calibration model improved the measurement accuracy by approximately 0.04% compared to the other two methods. Figure 7 shows that, regarding the root-mean-square error (RMSE), the combined calibration model reduced the RMSE by about 0.002 relative to the other two methods, reflecting the superior stability of this approach.

In summary, the compensation model based on combined heating–cooling calibration data

proposed in this study can effectively reduce the sensor output errors under rapid cooling conditions, thereby enhancing the operational stability of the sensors.

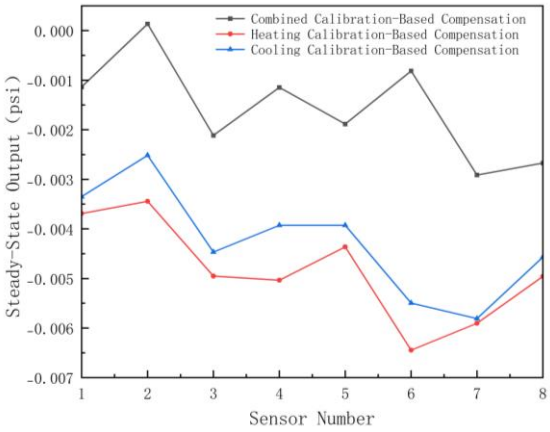

Figure 5. Steady-state outputs of the sensors during the cooling experiment

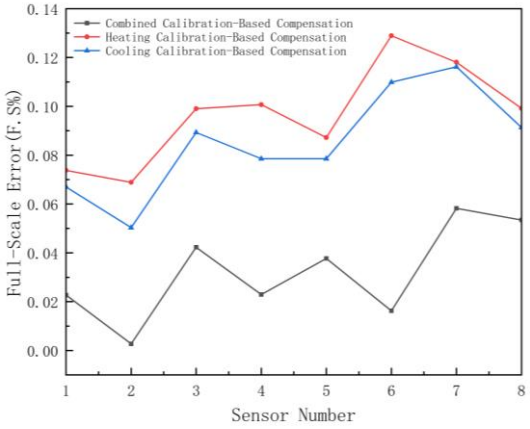

Figure 6. Full-scale errors of the sensors' steady-state outputs during the cooling experiment

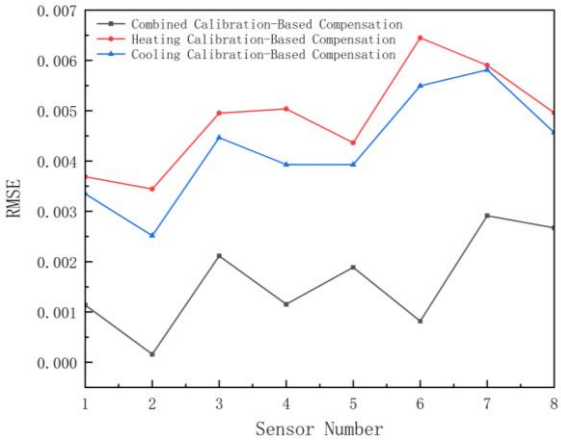

Figure 7. RMSE of the sensors' steady-state outputs during the cooling experiment

References

[1] Wang, Z. (2018). A brief discussion on the current status and development trends of MEMS pressure sensors. Science & Information Technology, (5), 84–85.
[2] Li, W., Wu, X., & Li, S. (2006). A piezoresistive micro-pressure sensor. Instrumentation Technology and Sensors, (7),

1–2, 5.
[3] Meng, H., & Gong, J. (2024). Application and development prospects of pressure sensors in industrial automation. Product Reliability Report, (09), 57–58.
[4] Yang, Q., & Wang, T. (2023). Nonlinearity error correction method for diffused silicon piezoresistive pressure sensors. Journal of Harbin Engineering University, 44(03), 466–472.
[5] He, H., Xu, J., Zhou, Z., et al. (2021). Study on interpolation compensation method for temperature errors of piezoresistive pressure sensors. Journal of Electronic Measurement and Instrumentation, 35(12), 1–7.
[6] Hu, F., Wang, B., Yang, H., et al. (2021). Effects of different ambient temperatures on barometric pressure sensors. Meteorological, Hydrological and Oceanographic Instruments, 38(02), 38–40.
[7] Falk, S., & Shi, L. (2025). A review of pressure sensor accuracy. Sensor World, 31(05), 6–10.